Available online at www.sciencedirect.com
ScienceDirect
Trans. Nonferrous Met. Soc. China 27(2017) 363−368
Transactions of Nonferrous Metals Society of China
www.tnmsc.cn

# Effect of minor Nb addition on mechanical properties of in-situ Cu-based bulk metallic glass composite

Hai-min ZHAI, Hai-feng WANG, Feng LIU

State Key Laboratory of Solidification Processing, Northwestern Polytechnical University, Xi'an 710072, China

Received 3 December 2015; accepted 14 June 2016

**Abstract:** In-situ formed $(Cu_{0.6}Zr_{0.3}Ti_{0.1})_{95}Nb_5$ bulk metallic glass (BMG) composite with Nb-rich dendrite randomly dispersed in hard glassy matrix was prepared by casting into a water-cooled copper mold. The dendrite has much smaller hardness and elastic modulus than glassy matrix, and the stress concentration at interface provides a channel for the initiating and branching of shear bands upon loading, thus leading to a high compressive fracture strain of 6.08% and fracture strength about 2200 MPa. Comparing with other Cu-based BMG composite, the fracture strength of present $(Cu_{0.6}Zr_{0.3}Ti_{0.1})_{95}Nb_5$ composite is not significantly reduced, indicating that the addition of Nb in the current work is an effective and effortless way to fabricate new practical BMG composites with enhanced strength and good plasticity.

**Key words:** bulk metallic glass composite; Nb addition; shear band; microstructure; mechanical property

## 1 Introduction

Bulk metallic glasses (BMGs) have been investigated extensively regarding their importance in science and engineering [1−3]. For this kind of featureless structure, however, the highly localized plastic flow in shear bands results in the occurrence of catastrophic failure by shear softening in certain bands. Therefore, BMGs have a limited amount of plasticity at ambient temperature [2,3]. In order to overcome this deficiency, much attention has been paid to the BMG composites which are formed by in-situ introducing a second ductile structure into hard glassy matrix. HAYS et al [4] developed a Zr−Ti−Nb−Cu−Ni−Be composite with in-situ formed BCC $\beta$-Ti dendrite which displays work hardening and a plastic strain of 6%−7%. This kind of composites have been manufactured widely in the Zr- [5,6], Cu- [7,8], Fe- [9] based BMGs. The excellent plasticity of the BMG composite is attributed to the homogeneous distributed dendrite whose size is equivalent to the length scale of the plastic deformation zone in glassy matrix [6]. The dendrite acts as an obstacle to bifurcate or impede shear banding, thus leading to a more uniform distribution of plastic strain and the improvement of plasticity.

Recently, synthesizing Cu-based BMGs achieve extensive research interests due to their high strength (exceeding 2000 MPa), lower cost and high glass-forming ability, offering the potential for wide application of these materials as engineering materials, such as in instruments and bipolar plates in fuel cells [1,10]. In order to improve the plasticity and toughness, many Cu-based BMG composites have been developed by in-situ formation of ductile body-centered cubic (BCC) phase [11,12]. To prevent the formation of brittle intermetallic compounds in these kinds of composites, some ductile refractory metals, such as Ta and Hf, are added because they can form extended solid solution with Zr and Ti. For example, QIN et al [11] prepared a Cu−Hf−Ti−Ta BMG composite that exhibits improved strength and compressive plasticity. Based on transmission electron microscopy (TEM) observations of the $(Cu_{60}Zr_{30}Ti_{10})_{0.95}Ta_{0.05}$ compression tests at ambient temperature, LEE et al [12] reported that the strengthening phenomenon of BMG composite in plastic

**Foundation item:** Project (51371149) supported by the National Natural Science Foundation of China; Project (151048) supported by the HUO Ying-dong Young Teacher Fund; Project (2015ZF53066) supported by the Aeronautical Science Foundation of China; Project (92-QZ-2014) supported by the Free Research Fund of State Key Laboratory of Solidification Processing, China; Project (2015KJXX-10) supported by Shaanxi Young Stars of Science and Technology, China; Proejct (2011CB610403) supported by the National Basic Research Program of China; Project (51125002) supported by the National Science Funds for Distinguished Young Scientists,China

**Corresponding author:** Hai-feng WANG; Tel: +86-29-88460311; E-mail: haifengw81@nwpu.edu.cn; LIU Feng; Tel: +86-29-88460374; E-mail: liufeng@nwpu.edu.cn

DOI: 10.1016/S1003-6326(17)60040-2

regime is due to the homogeneous precipitation of nanocrystallites in glassy matrix. The high melting point and high-cost, however, limit the preparation and application of this kind of composite with Ta element.

In this work, a $(Cu_{0.6}Zr_{0.3}Ti_{0.1})_{95}Nb_5$ BMG composite with in-situ formed dendrite was prepared. The ternary $Cu_{60}Zr_{30}Ti_{10}$ BMG was selected as the base alloy because of its high glass forming ability [13]. Nb with a positive mixing enthalpy with Cu, Zr and Ti elements, was chosen as the addition element due to its high melting point, further rendering the precipitation from the liquid upon cooling. Furthermore, HOFMANN et al [14] attributed the significant tensile ductility to the crystalline inclusion which has a lower shear modulus than glassy matrix. Noting that the Nb element has a lower shear modulus than the Ta element, it may be a good choice for improving the plasticity. Using the energy-dispersive spectroscope (EDS) and indentation technique, the composition and mechanical properties of dendrite and glassy matrix were investigated. The compression tests were carried out to show the deformation mechanism.

## 2 Experimental

Ingots of nominal compositions of $Cu_{60}Zr_{30}Ti_{10}$ and $(Cu_{0.6}Zr_{0.3}Ti_{0.1})_{95}Nb_5$ (mole fraction, %) were prepared on a water-cooled copper hearth by arc-melting the mixture of Cu, Zr, Ti or/and Nb with purity better than 99.9% (mass fraction) under a Ti-gettered argon atmosphere. The ingots were re-melted at least four times to ensure the compositional homogeneity. Both the $Cu_{60}Zr_{30}Ti_{10}$ and the $(Cu_{0.6}Zr_{0.3}Ti_{0.1})_{95}Nb_5$ BMG composites were prepared by injecting the melts into a copper mold, forming cylindrical rods with a diameter of 1.5 mm. The phases in the as-cast alloys were identified by the X-ray diffraction (XRD: Panalytical X'pert MPD Pro) with a Cu $K_\alpha$ radiation. The microstructures were further analyzed by TEM (Tecnai G2 F30, 300 kV) and scanning electron microscopy (SEM: TESCAN VEGA 3 LMU, JSM−6390A). The compositions of dendrite and glassy matrix were analyzed by EDS (Oxford, X-Max 20). The quasi-static compression tests were carried out on a universal testing machine (Instron 3382) at an engineering strain rate of $1\times10^{-4}$ $s^{-1}$. The compression samples were prepared with a diameter of 1.5 mm and a length of 3 mm. The nanoindentation test samples were mechanically polished and then cleaned by high purity ethanol. The indentation tests were carried out with a Berkovich diamond indenter (Nano Indenter XP, MTS). To compare the mechanical properties of dendrite with glassy matrix, all the samples were indented at the same load-indentation depth of 2000 nm. In order to obtain accurate measurements of dendrite, only the results that indent exactly within the dendrite were adopted. For each sample, 10 indentations were performed to obtain the averaged hardness and elastic modulus. In order to demonstrate the interaction between dendrite and shear bands under the loading conditions, the as-cast samples were indented by a series of Vickers hardness tests with a load of 19.6 N for 3 min.

## 3 Results and discussion

### 3.1 Microstructure and composition

Figure 1(a) shows the SEM image of as-cast $(Cu_{0.6}Zr_{0.3}Ti_{0.1})_{95}Nb_5$ BMG composite, where the precipitated phase (volume fraction of 8%) has a dendritic morphology with a size ranging from 10 to 50 μm and appears to disperse randomly in glassy matrix. The composite structure is evidenced by the XRD pattern (inset of Fig. 1(a)), exhibiting a typical broad hump and some sharp crystalline peaks (indexed as Nb phase), as compared to the fully amorphous structure in as-cast $Cu_{60}Zr_{30}Ti_{10}$ alloy. Figure 1(b) shows a typical high-resolution transmission electron microscopy (HRTEM) image of the area near the boundary between dendrite and glassy matrix, where the diffuse diffraction ring and periodic diffraction spots of selected area

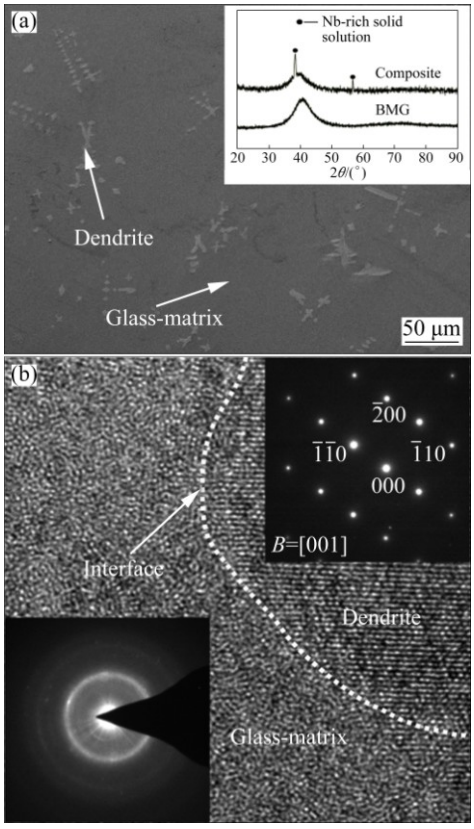


**Fig. 1** SEM image and XRD patterns (inset) of $Cu_{60}Zr_{30}Ti_{10}$ BMG and $(Cu_{0.6}Zr_{0.3}Ti_{0.1})_{95}Nb_5$ BMG composite (a) and HRTEM image of $(Cu_{0.6}Zr_{0.3}Ti_{0.1})_{95}Nb_5$ BMG composite with corresponding SEAD patterns of dendrite and glassy matrix (b)

electron diffraction (SAED) patterns correspond to the nature of glass and crystal (inset in Fig. 1(b)), respectively. The dendrite is further indexed as BCC phase, conclusively, indicating the precipitation of Nb-rich dendrite from the melts upon cooling.

The compositions of the dendrite and glassy matrix in the $(Cu_{0.6}Zr_{0.3}Ti_{0.1})_{95}Nb_5$ BMG composite were analyzed by EDS. The dendrite composition seriously deviates from the nominal composition and presents a solid-solution phase enriched in Nb (79.91%, mole fraction) and Ti (14.53%, mole fraction). It is noted that Nb has positive mixing enthalpies of 3, 4 and 2 kJ/mol with Cu, Zr and Ti, respectively [15]; Zr has the largest atom size among the component elements (the atomic size: $r_{Zr}$=0.160 nm, $r_{Ti}$=0.147 nm, $r_{Nb}$=0.146 nm and $r_{Cu}$=0.128 nm[16]). This indicates that it is very difficult for the Zr element to dissolve into Nb crystalline structure due to its large atomic size and maximal positive mixing enthalpy with Nb. The atomic size of Ti is close to that of Nb and their mixing enthalpy is the smallest one. Therefore, the Ti content in dendrite should be much higher than the contents of the Cu and Zr elements. The highest melting point of Nb (Nb 2750 K, Cu 1357.77 K, Zr 2127.85 K and Ti 1941 K [17]) is also responsible for the enrichment of Nb and Ti in solid-solution dendrite.

### 3.2 Mechanical properties

The engineering stress−strain curves of the $Cu_{60}Zr_{30}Ti_{10}$ BMG and $(Cu_{0.6}Zr_{0.3}Ti_{0.1})_{95}Nb_5$ BMG composites under the quasi-static compression with a diameter of 1.5 mm are shown in Fig. 2. The yielding strength ($\sigma_y$), yielding strain ($\varepsilon_y$), fracture strength ($\sigma_f$) and fracture strain ($\varepsilon_f$) of the $Cu_{60}Zr_{30}Ti_{10}$ BMG and $(Cu_{0.6}Zr_{0.3}Ti_{0.1})_{95}Nb_5$ BMG composite are listed in Table 1. For the $Cu_{60}Zr_{30}Ti_{10}$ BMG, the sample fractured immediately after compression strength reached 2025.52 MPa. For the $(Cu_{0.6}Zr_{0.3}Ti_{0.1})_{95}Nb_5$ BMG composite, the samples have an obvious plasticity after yielding at 1798.09 MPa and with a fracture strain of 6.08%. Comparing $Cu_{60}Zr_{30}Ti_{10}$ BMG with $(Cu_{0.6}Zr_{0.3}Ti_{0.1})_{95}Nb_5$ BMG composite, the fracture strain increases from 1.92% to 6.08%. This result indicates clearly that the mechanical properties of Cu-based BMGs were improved by the dispersion of ductile dendritic phase, which is consistent with the studies in Ta-bearing BMGs composites [11,12]. For the $(Cu_{0.6}Zr_{0.3}Ti_{0.1})_{99}Ta_1$ BMG, it has a high fracture strength about 2250 MPa. With the increase of the Ta content to 5% (mole fraction), the $(Cu_{0.6}Zr_{0.3}Ti_{0.1})_{95}Ta_5$ BMG composite formed, which has a high fracture strength about 2332 MPa. Despite the substitution of Ta by Nb, the present $(Cu_{0.6}Zr_{0.3}Ti_{0.1})_{95}Nb_5$ BMG composite has a comparable fracture strength as compared with Ta-bearing BMG composites.

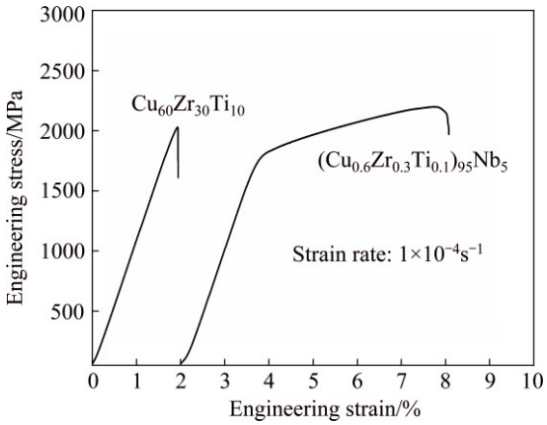


**Fig. 2** Compressive engineering stress−strain curves of $Cu_{60}Zr_{30}Ti_{10}$ BMG and $(Cu_{0.6}Zr_{0.3}Ti_{0.1})_{95}Nb_5$ BMG composite

**Table 1** Compressive mechanical properties of $Cu_{60}Zr_{30}Ti_{10}$ BMG and $(Cu_{0.6}Zr_{0.3}Ti_{0.1})_{95}Nb_5$ BMG composite

| Alloy | $\sigma_y$/MPa | $\varepsilon_y$/% | $\sigma_f$/MPa | $\varepsilon_f$/% |
|---|---|---|---|---|
| $Cu_{60}Zr_{30}Ti_{10}$ | − | − | 2025.52 | 1.92 |
| $(Cu_{0.6}Zr_{0.3}Ti_{0.1})_{95}Nb_5$ | 1798.09 | 1.86 | 2203.15 | 6.08 |

Figure 3 shows the fracture surfaces of the $Cu_{60}Zr_{30}Ti_{10}$ BMG and $(Cu_{0.6}Zr_{0.3}Ti_{0.1})_{95}Nb_5$ BMG composite. The $Cu_{60}Zr_{30}Ti_{10}$ BMG failed in a typical brittle manner with few shear bands on the lateral surface (Fig. 3(a)). The fracture surface of the $Cu_{60}Zr_{30}Ti_{10}$ BMG presents the river-like vein pattern originating from shear deformation (Fig. 3(b)). Due to the BMG having a high elastic strain [18], there will be a high elastic strain energy density of the sample upon deformation. Then these elastic strain energies will be dissipated in the thin shear bands, rather than the entire sample. Therefore, the temperature will rise sharply in the shear bands [19] and lead to shear softening and fracture accompanying with vein patterns on the fracture surface. Compared with the $Cu_{60}Zr_{30}Ti_{10}$ BMG, the lateral fracture of the $(Cu_{0.6}Zr_{0.3}Ti_{0.1})_{95}Nb_5$ BMG composite presents different characteristics (Fig. 3(c)), where abundant primary shear bands and secondary shear bands distribute on the lateral surface of sample. The random distribution of shear bands without a fixed propagating direction suggests a uniform deformation of the BMG composite. Its fracture surface exhibits resolidified liquid droplets accompanying with vein patterns (Fig. 3(d)).

### 3.3 Nanoindentation tests

Since there is a clear boundary between dendrite and glassy matrix, it is possible to investigate their mechanical properties by nanoindentation tests [20,21]. The hardness−displacement curves (the evolution of hardness with contact depth) are shown in Fig. 4(a). The average hardnesses of the glassy matrix, dendrite and

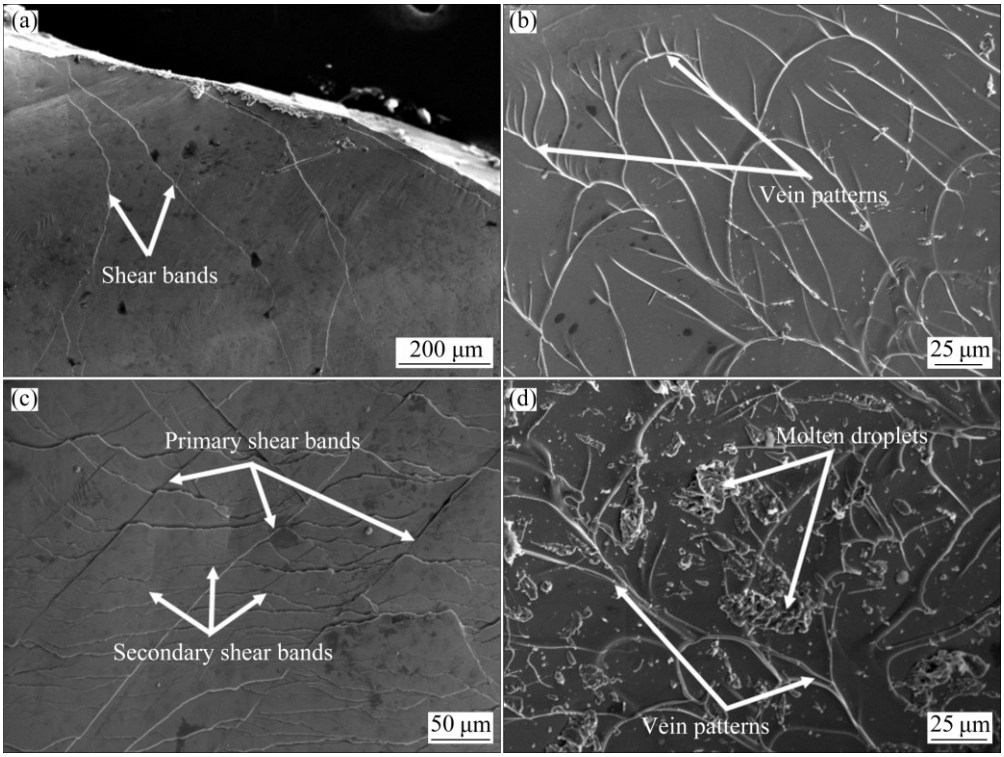


**Fig. 3** Lateral surface (a, c) and fracture surface (b, d) of $Cu_{60}Zr_{30}Ti_{10}$ BMG and $(Cu_{0.6}Zr_{0.3}Ti_{0.1})_{95}Nb_5$ BMG composite, respectively

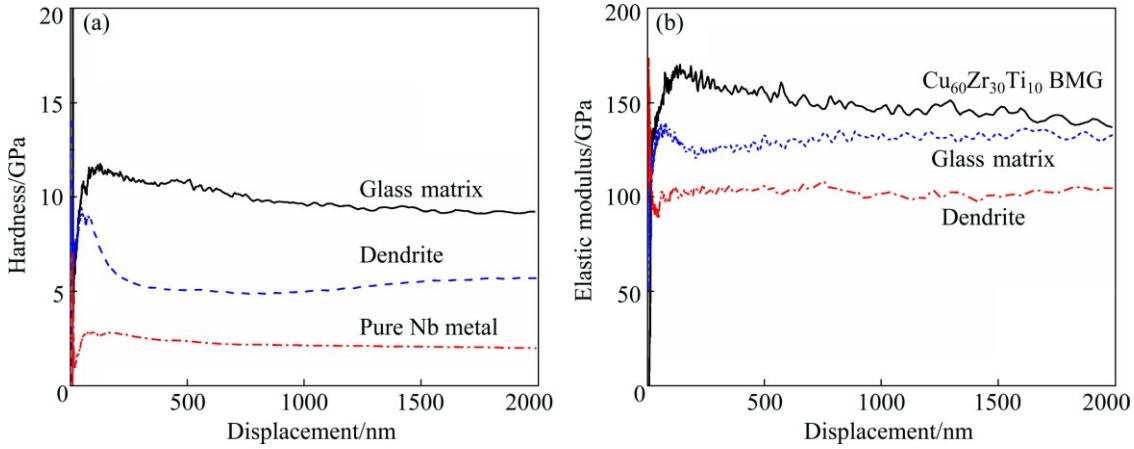


**Fig. 4** Hardness−displacement curves for pure Nb, dendrite and glassy matrix in $(Cu_{0.6}Zr_{0.3}Ti_{0.1})_{95}Nb_5$ BMG composite (a), and elastic modulus−displacement curves for $Cu_{60}Zr_{30}Ti_{10}$ BMG, glassy matrix and dendrite in $(Cu_{0.6}Zr_{0.3}Ti_{0.1})_{95}Nb_5$ BMG composite (b)

pure Nb metal are 12.28, 6.93 and 2.078 GPa, respectively. It is easy to see that the hardness of dendrite is three times of pure Nb metal due to solution strength. Figure 4(b) shows the elastic modulus−displacement curves (the evolution of elastic modulus with contact depth). The average elastic moduli of the dendrite and glassy matrix in $(Cu_{0.6}Zr_{0.3}Ti_{0.1})_{95}Nb_5$ BMG composite and $Cu_{60}Zr_{30}Ti_{10}$ BMG are 112.3, 128.1 and 164.6 GPa, respectively, namely, the dendrite precipitation results in the decrease of elastic modulus. Nb has a positive mixing enthalpy with other component elements; it is difficult for Nb to form strong chemical bonding with other elements and to have a densely packed structure, which corresponds to a small elastic modulus [22].

### 3.4 Evolution of shear bands

In order to clarify how the dendrite interacts with shear bands and contributes to the plasticity, a Vickers hardness test was carried out. Figure 5 shows the SEM images of the indent on BMG composite. Under the deformation of indent loading, the shear bands form in glassy matrix. It can be seen that the shear bands propagate and bifurcate through glassy matrix and interact with dendrite (Fig. 5). The dendrite phase effectively impedes the rapid propagation of shear bands, and then induces branches and multiplication of shear

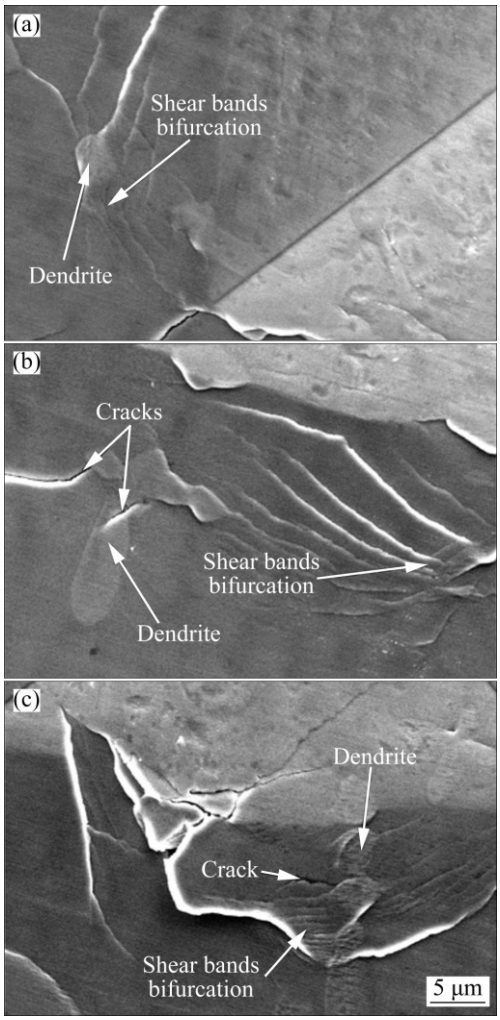


**Fig. 5** SEM images of indent on glassy matrix in $(Cu_{0.6}Zr_{0.3}Ti_{0.1})_{95}Nb_5$ composite: (a) Shear bands bifurcation; (b) Shear bands hindering by dendrite; (c) Shear bands migrating across dendrite

bands at the interface between the dendrite and glassy matrix. Upon severe plastic deformation, the crack forms in glassy matrix and propagates through these shear bands. The crack grows along the matrix/dendrite boundary or across the dendrite (Figs. 5(b) and (c)). When the crack density exceeds the limitation of dendrite accommodated, fracture happens. Together with Figs. 3(a) and (c), during the loading deformation, the migratory primary shear bands propagate through glassy matrix and interact with dendrite, and then are hindered by the soft dendrite. In order to bear deformation, the shear bands have to bifurcate to change their propagating direction and form abundont secondary shear bands in glassy matrix, thus greatly improving the plasticity of BMG composites.

It is well accepted that the metallic glass without any defects is not capable of plastic flow [23]. For in-situ BMG composite, the dendrite firstly deformed because of its lower elastic modulus and yielding strength upon loading. Since the stress concentration at the interface can provide a channel for the initiation of shear bands, the plastic strain can be accommodated by shear bands within glassy matrix and the dislocations within dendrites. The dendrite thus can inhibit the rapid propagation of shear bands. Further deformation needs to initiate new shear bands. From Fig. 4(a), under loading of the nanoindent, the hardness of glassy matrix gradually increases when the displacement exceeds 1000 nm. The work-hardening in dendrite appears because of the existence of dislocations upon drastically plastic deformation [24−26]. Compared with $(Cu_{0.6}Zr_{0.3}Ti_{0.1})_{95}Ta_5$ BMG composite, the present $(Cu_{0.6}Zr_{0.3}Ti_{0.1})_{95}Nb_5$ BMG composite has a higher work-hadening ability (Compression strength increases from about 1800 to 2200 MPa with 6.08% fracture strain). Meanwhile, the $(Cu_{0.6}Zr_{0.3}Ti_{0.1})_{95}Nb_5$ BMG composite can be esaily prepared due to a relatively low melting point of Nb.

## 4 Conclusions

1) The $(Cu_{0.6}Zr_{0.3}Ti_{0.1})_{95}Nb_5$ BMG composite with a random distribution dendrite structure was prepared. The dendrite has higher hardness than the pure Nb metal because of the solid solution strengthening effect.

2) The addition of the Nb element into $Cu_{60}Zr_{30}Ti_{10}$ BMG significantly increases the strength and plasticity, and leads to the $(Cu_{0.6}Zr_{0.3}Ti_{0.1})_{95}Nb_5$ BMG composite with a high compression fracture strength of about 2200 MPa and compression fracture strain of 6.08%.

3) Under the deformation, the ductile dendrite acts as the sites for the arrest barriers of shear bands, and also induces the formation of multiple shear bands.

4) Since the Nb element has lower melting point and cost as compared with Ta element, the substitution of Ta by Nb in the present work is of practical implication.

## References

[1] INOUE A, TAKEUCI A. Recent development and application products of bulk glassy alloys [J]. Acta Mater, 2011, 59: 2243−2267.

[2] SCHUH C A, HUFNAGEL T C, RAMAMURTY U. Mechanical behavior of amorphous alloys [J]. Acta Mater, 2007, 55: 4067−4109.

[3] DAS J, TANG M B, KIM K B, THEISSMANN R, BAIER F, WANG W H, ECKERT J. “Work-hardenable” ductile bulk metallic glass [J]. Phys Rev Lett, 2005, 94: 205501−4.

[4] HAYS C C, KIM C P, JOHNSON W L. Microstructure controlled shear band pattern formation and enhanced plasticity of bulk metallic glasses containing in situ formed ductile phase dendrite dispersions [J]. Phys Rev Lett, 2000, 84: 2901−2904.

[5] TAMURA T, MAKAYA A, MIWA K. Application of semisolid process to Zr-based metallic glass matrix composites [J]. Transactions of Nonferrous Metals Society of China, 2010, 20: 719−722.

[6] QIAO JW, FENG P, ZHANG Y, ZHANG Q M, CHEN G L.

Quasi-static and dynamic deformation behaviors of Zr-based bulk metallic glass composites fabricated by the Bridgman solidification [J]. J Alloys Compd, 2009, 486: 527−531.
[7] KIM Y C, KIM D H, LEE J C. Formation of ductile Cu-based bulk metallic glass matrix composite by Ta addition [J]. Mater Trans, 2003, 44: 2224−2227.
[8] PAULY S, LIU G, WANG G, KUHN U, MATTERN N, ECKERT J. Microstructural heterogeneities governing the deformation of Cu47.5Zr47.5Al5 bulk metallic glass composites [J]. Acta Mater, 2009, 57: 5445−5453.
[9] GUO Sheng-feng, WANG Jing-feng, ZHANG Hong-ju, XIE Sheng-hui. Enhanced plasticity of Fe-based bulk metallic glass by tailoring microstructure [J]. Transactions of Nonferrous Metals Society of China, 2012, 22: 348−353.
[10] XU Hong-wei, DU Yu-lei, DENG Yu. Effects of Y addition on structural and mechanical properties of CuZrAl bulk metallic glass [J]. Transactions of Nonferrous Metals Society of China, 2012, 22: 842−846.
[11] QIN C L, ZHANG W, KIMURA H, INOUE A. Excellent mechanical properties of Cu−Hf−Ti−Ta bulk glassy alloys containing in-situ dendrite Ta-based BCC phase [J]. Mater Trans, 2004, 45: 2936−2940.
[12] LEE J C, KIM Y C, AHN J P, LEE S, LEE B J. Strain hardening of an amorphous matrix composite due to deformation-induced nanocrystallization during quasi-static compression [J]. Appl Phys Lett, 2004, 84: 2781−2783.
[13] ZHANG T, KUROSAKA K, INOUE A. Thermal and mechanical properties of Cu-based Cu−Zr−Ti−Y bulk glassy alloys [J]. Mater Trans, 2001, 42: 2042−2045.
[14] HOFMANN D C, SUH J Y, WIEST A, DUAN G, LIND M L, DEMETRIOU MD. Designing metallic glass matrix composites with high toughness and tensile ductility [J]. Nature, 2008, 451: 1085−1089.
[15] BIAN Z, KATO H, QIN C L, ZHANG W, INOUE A. Cu−Hf−Ti−Ag−Ta bulk metallic glass composites and their properties [J]. Acta Mater, 2005, 53: 2037−2048.
[16] MIRACLE D B. The efficient cluster packing model—An atomic structural model for metallic glasses [J]. Acta Mater, 2006, 54: 4317−4336.
[17] DINSDALE A T. SGTE data for pure elements [J]. Calphad, 1991, 15: 317−425.
[18] KETOV S V, LOUZGUIN-LUZGIN D V. Localized shear deformation and softening of bulk metallic glass: Stress or temperature driven? [J]. Sci Rep, 2013, 3: 2978.
[19] ASHBY M F, GREER A L. Metallic glasses as structural materials [J]. Scripta Mater, 2006, 54: 321−326.
[20] SONG Zhong-kang, MA De-jun, GUO Jun-hong, CHEN Wei. A modified method of nanoindentation testing method [J]. Transactions of Nonferrous Metals Society of China, 2012, 22: 520−525.
[21] DONG He, ZHU Jing-chuan, LAI Zhong-hong, LIU Yong, YANG Xia-wei, NONG Zhi-sheng. Residual elastic stress-strain field and geometrically necessary dislocation density distribution around nanoindentation in TA15 titanium alloy [J]. Transactions of Nonferrous Metals Society of China, 2013, 23: 7−13.
[22] INOUE A, ZHANG W, ZHANG T, KUROSAKA K. High-strength Cu-based bulk glassy alloys in Cu−Zr−Ti and Cu−Hf−Ti ternary systems [J]. Acta Mater, 2001, 49: 2645−2652.
[23] SCHUH C A, NIEH T G. A nanoindentation study of serrated flow in bulk metallic glasses [J]. Acta Mater, 2003, 51: 87−99.
[24] LIU Hui-qun, YI Dan-qing, WANG Wei-qi, WANG Li-ping, LIAN Cai-hao. Influence of Sc on high temperature strengthening behavior of Ti−6A1−4V alloy [J]. Transactions of Nonferrous Metals Society of China, 2007, 17: 1212−1219.
[25] REN Jiang-wei, SHAN Ai-dang. Strengthening and stress drop of ultrafine grain aluminum after annealing [J]. Transactions of Nonferrous Metals Society of China, 2010, 20: 2139−2142.
[26] RIM K R, PARK J M, KIM W T, KIM D H. Tensile necking and enhanced plasticity of cold rolled $\beta$-Ti dendrite reinforced Ti-based bulk metallic glass matrix composite [J]. J Alloys Compd, 2013, 579: 253−258.

# 微量添加 Nb 元素对原位合成 Cu 基非晶复合材料力学性能的影响

翟海民，王海丰，刘 峰

西北工业大学 凝固技术国家重点实验室，西安 710072

**摘 要：**利用铜模铸造法获得$(Cu_{0.6}Zr_{0.3}Ti_{0.1})_{95}Nb_5$块体非晶复合材料试样。该试样中均匀分布富 Nb 元素的枝晶相。结果表明，相比于非晶基体，枝晶具有更低的硬度值和弹性模量，在加载变形过程中，非晶基体和枝晶界面处产生应力集中，促使非晶基体中剪切带的萌生和分叉增殖，最终获得了约 2200 MPa 的压缩断裂强度和 6.08%断裂应变。与其他 Cu 基非晶复合材料相比，所制备的$(Cu_{0.6}Zr_{0.3}Ti_{0.1})_{95}Nb_5$非晶复合材料断裂强度没有明显的降低，证明添加 Nb 元素是一种非常容易和有效制备实用高强度、高塑性非晶复合材料的方法。

**关键词：**块体非晶复合材料；Nb 添加；剪切带；组织；力学性能

**(Edited by Xiang-qun LI)**